

Contents lists available at [ScienceDirect](https://www.sciencedirect.com)

Journal of Hydrology

journal homepage: [www.elsevier.com/locate/jhydrol](http://www.elsevier.com/locate/jhydrol)

Research papers

# Spatial coherency of the spring flood signal among major river basins of eastern boreal Canada inferred from flood rings

A.F. Nolin<sup>a,b,c,\*</sup>, J.C. Tardif<sup>b,c,2</sup>, F. Conciatori<sup>b</sup>, Y. Bergeron<sup>a,c,3</sup><sup>a</sup> Institut de Recherche sur les Forêts, Université du Québec en Abitibi-Témiscamingue (UQAT), Rouyn-Noranda, Québec J9X 5E4, Canada<sup>b</sup> Centre for Forest Interdisciplinary Research (C-FIR), University of Winnipeg, Department of Biology/Environmental Studies & Sciences, 515 Avenue Portage, Winnipeg, Manitoba R3B 2E9, Canada<sup>c</sup> Centre d'Étude de la Forêt, Université du Québec à Montréal (UQAM), CP 8888, Succ. A Montréal, Montréal, Québec H3C 3P8, Canada

## ARTICLE INFO

This manuscript was handled by Marco Borga, Editor-in-Chief

## Keywords:

*Fraxinus nigra*  
Spring floods  
Earlywood vessels  
Lake Duparquet  
Dendrohydrology  
Flood ring

## ABSTRACT

In eastern boreal Canada, long-term perspective in water resources and hydroelectric dam management is currently limited by the lack of long-term hydrological records. The research for new paleohydrological proxies would help fill this hydrological data gap and provide regional hydroclimatic predictive trajectories in the context of climate change. The development of long annually resolved series of earlywood vessel cross-sectional area has recently demonstrated a high potential for reconstructing high and low discharges. This study analyzes a network of 10 sites scattered around Lake Duparquet. The region covers an area of about 20 000 km<sup>2</sup> including four river basins characterized by natural and regulated rivers, and unflooded control sites. The objectives were to assess 1) the spatial coherency in flood-rings chronologies among sites and Lake Duparquet, and among hydrological regimes (natural, regulated and unflooded control) and 2) their degree of association with i) annually resolved chronologies of earlywood vessel cross-sectional area and number, ii) a reconstruction of the Harricana River spring discharge and iii) discharge data from eleven hydrometric stations distributed in the study area. It was hypothesized that flood rings would be consistent among natural rivers and absent from regulated rivers. Results showed high spatial coherency among natural rivers with flood rings recording the major floods of the last 250 years. Flood ring and earlywood vessel chronologies were strongly correlated to both reconstructed and instrumental discharge data. On regulated rivers, trees were younger than at the other sites and mainly spring floods that occurred prior to dam creation and the few extreme floods after dam creation were recorded by flood rings. One hypothesis is that older trees (before dam) most likely recorded the natural dynamic of the river, while younger trees (after dam) most likely recorded dam management maneuvers and spring flood exceeding dam capacity. Flood rings and earlywood vessel chronologies provided comparable and complementary hydrological evidence. Flood rings were easily identified visually allowing fast determination of major flood years whereas developing earlywood vessel chronologies, while being more tedious and time consuming, allowed capturing a larger spectrum of hydrological conditions

## 1. Introduction

The hydrological variability observed in recent decades worldwide is unusual and raises questions about the potential impacts of climate change on water resources (IPCC, 2018). Worldwide, exceptional floods and droughts are becoming more frequent and intense and are expected

to become even more severe under a warmer climate (Berghuijs et al., 2017; Kundzewicz et al., 2019). In Canada, the severity of floods in the last decade is unprecedented on the scale of 20<sup>th</sup> century hydrological records (Burn and Whitfield, 2016; Gaur et al., 2018). The Insurance Bureau of Canada for Natural Disaster reports nearly \$1 billion Canadian dollars spent annually on insurance payouts since 2010 (IBC, 2020). For

\* Corresponding author at: Institut de Recherche sur les Forêts, Université du Québec en Abitibi-Témiscamingue (UQAT), Rouyn-Noranda, Québec J9X 5E4, Canada.

E-mail address: [alexandreflorent.nolin@uqat.ca](mailto:alexandreflorent.nolin@uqat.ca) (A.F. Nolin).

<sup>1</sup> ORCID: 0000-0003-1033-9123.

<sup>2</sup> ORCID: 0000-0002-0145-9898.

<sup>3</sup> ORCID: 0000-0003-3707-3687.

<https://doi.org/10.1016/j.jhydrol.2021.126084>

Received 26 November 2020; Received in revised form 2 February 2021; Accepted 13 February 2021

Available online 20 February 2021

0022-1694/© 2021 Elsevier B.V. All rights reserved.

example, the 2019 flood in the Ottawa River basin exceeded that of 2017 which was considered the 100-year flood (ECCC, 2020).

Since the 1950's northern Canada has warmed by an annual average of 2.3°C and total annual precipitation has increased by +35% (Zhang et al., 2000; Bush and Lemmen, 2019). Global warming directly affects seasonal flows in the boreal region because of snow and discharge interactions. The most significant changes observed from 1950 were in winter where the combination of changes in temperature and precipitation over snow cover resulted in higher winter discharges (Vincent et al., 2015; Mudryk et al., 2018; Aygün et al., 2019; Bush and Lemmen, 2019). Episodes of rain-on-snow or rain-in-place of snow, and mid-winter thaws feed winter discharge in the boreal rivers instead of storing water in the snow cover. Instrumental records of the past century in Canada also have shown a reduction in spring discharge and in summer discharge associated with a shorter ice season (Aygün et al., 2019; Bush and Lemmen, 2019).

Hydrological trends across Canada, however, show high spatial variability which mainly relates to complex climate and discharge interactions, regional landscape complexities and the lack of long-term hydrological data (Mortsch et al., 2015; Aygün et al., 2019; Bush and Lemmen, 2019). In fact, most of the historical hydrometric stations in both northern Québec and Ontario were installed at the time of the creation of the hydroelectric generating stations which complicate the comparison of hydrological records between the pre- and post-dam periods (Supp. Table 1). It also remains uncertain how the projected climate change will affect the frequency and magnitude of extreme floods and droughts (Gaur et al., 2018). Hydrological simulations for northern Manitoba, Ontario and Québec estimated the magnitude of the change in the probable maximum flood to be between -1.5 and +21% by 2070 (Clavet-Gaumont et al., 2017). The estimated 100-year snowpack variations ranged from -9% to +8% with large variations between the southern and northern parts of the provinces. Similarly, the simulations for Québec predict earlier spring floods and an increase in winter and mean annual discharge with a strong intensity gradient from south to north (Guay et al., 2015).

Projected changes in hydrological regimes will also affect the management of hydroelectric facilities, particularly in northern Canada (Boucher and Leconte, 2013; Cherry et al., 2017). One of the major issues concerns the stability of dams throughout their lifespan given that Canada's major facilities were built to last more than 100 years (Clavet-Gaumont et al., 2017). For Québec, where more than 95% of the energy demand is supplied by hydropower with sales representing more than \$2.9 billion Canadian dollars per year, considering mitigation and adaptation scenarios is essential (Hydro-Québec, 2020).

Paleoclimatic proxy data have played an important role in extending hydroclimate records to help in planning for future water resource variability. Applications of tree-ring science to hydrology have allowed, among others, to extend instrumental discharge records in time (Meko and Woodhouse, 2011; Boucher et al., 2011; Nolin et al., 2021). Proxy derived from annually resolved tree rings have been used to extend times series of precipitation (Griffin et al., 2013), discharge (Agafonov et al., 2016; Nolin et al., 2021), drought (Biondi and Meko, 2019), or lake levels (Tardif and Bergeron, 1997b; Bégin, 2001; Tardif et al., 2010), while few have assessed their potential for flood reconstruction (St-George and Nielsen, 2003; Tardif et al., 2010; Kames et al., 2016; Nolin et al., 2021).

In recent years, flood rings that form in tree rings from riparian ring-porous species has allowed to identify major spring floods in various river basins and prior to instrumental records (St. George and Nielsen, 2000, 2003; Tardif et al., 2010; Wertz et al., 2013; Therrell & Bialecki, 2015; Kames et al., 2016; Meko & Therrell, 2020). In ring-porous tree species (e.g., *Quercus* and *Fraxinus*), flood rings are characterized by increased earlywood vessel density and/or reduced earlywood vessel cross-sectional areas (St. George and Nielsen, 2003; Tardif et al., 2010; Copini et al., 2016; Kames et al., 2016; Nolin et al., 2021). Anatomical changes in earlywood vessels occur in the submerged portion of the tree

stem if flooding happens to coincide with the period of active earlywood formation (St. George et al., 2002; Copini et al., 2016). At Lake Duparquet in northwestern Québec, chronologies of earlywood vessels from black ash trees (*Fraxinus nigra* Marsh.) better reflected spring discharge variability than tree-ring widths (Kames et al., 2016) and were successfully used to reconstruct Harricana River spring discharge from 1771 to 2016 (Nolin et al., 2021).

In contrast to flood studies conducted at Lake Duparquet (Tardif et al., 2010; Kames et al., 2016; Nolin et al., 2021) or the Red River (St. George and Nielsen, 2000, 2003), the use of flood rings in North America could be spatially hindered in areas where electricity generation has resulted in river regulation. Dam management alters the natural availability of water in terms of mean seasonal levels and frequency of flooding which in turn affect riparian forests (Stella and Bendix, 2019) and possibly their use as discharge proxy. In regulated rivers, correlations between tree-ring width chronologies and discharge tend to decrease whereas those with precipitation tend to increase resulting in a decreased effectiveness in reconstructing discharge (Reily and Johnson, 1981; Schook et al., 2016; Netsvetov et al., 2019). Up to now, no studies have assessed the impact of discharge regulation on flood-rings formation in riparian trees.

The objectives of this study were twofold. First, the spatial coherency in flood-ring chronologies was assessed among a network of ten sites located along four river basins in northeastern Canada (Mattagami, Abitibi, Harricana and upper Ottawa Rivers) and at Lake Duparquet, and under three different hydrological regimes (natural, regulated and at unflooded control). It was hypothesized that the flood-ring chronologies among natural river basins will be similar and that they will differ from those originating from regulated rivers, especially after the creation of dams. Second, we determined the degree of association between flood-ring chronologies and i) continuous annually resolved series of earlywood vessel cross-sectional area and number, ii) a reconstruction of the Harricana River spring discharge and iii) discharge data from eleven hydrometric stations distributed in the study area. It was hypothesized that these various datasets will be highly correlated thus illustrating the large-scale spatial coherency in the spring flood signal in eastern boreal Canada.

## 2. Material and methods

### 2.1. Study area

The study area encompasses Lake Duparquet and four major river basins (Mattagami, Abitibi, Harricana and upper Ottawa Rivers) located in northeastern Canada (Fig. 1). It roughly covers an area of about 20 000 km<sup>2</sup>. The Mattagami, Abitibi and Harricana Rivers are flowing north and are major southern tributaries of the James Bay in the Hudson sea (Déry et al., 2011) while the upper Ottawa River is flowing south to the Saint-Lawrence estuary (Figure 1). Lake Duparquet (48°28'N; 79°16'W) is situated in the upstream section of the Abitibi River, near the continental divide (Fig. 1). The Mattagami and Abitibi Rivers are partially regulated with dams implanted since the 1910s (CEHQ, 2019; OMNRF, 2019; Supp. Table 1) while the Harricana and upper Ottawa Rivers are naturally flowing (CEHQ, 2019; OMNRF, 2019). The regional hydrological regime is dominated primarily by snowmelt and summer precipitation, with most of the annual discharge flowing during the spring breakup flood. For example, the mean discharge of the Harricana River in May represents 11 to 30% of the total annual discharge over the period 1915–2020 (Nolin et al., 2021).

The study area is part of the northern clay belt of Québec and Ontario where the soils are dominated by glacio-lacustrine deposits that transform into peatlands northward (Daubois et al., 2015). It is also the southern limit of the boreal forest where mixedwood associations are composed of balsam fir (*Abies balsamea* (L.) Mill.), black spruce (*Picea mariana* (Mill.) BSP), paper birch (*Betula papyrifera* Marsh.), white spruce (*Picea glauca* (Moench) Voss) and trembling aspen (*Populus*

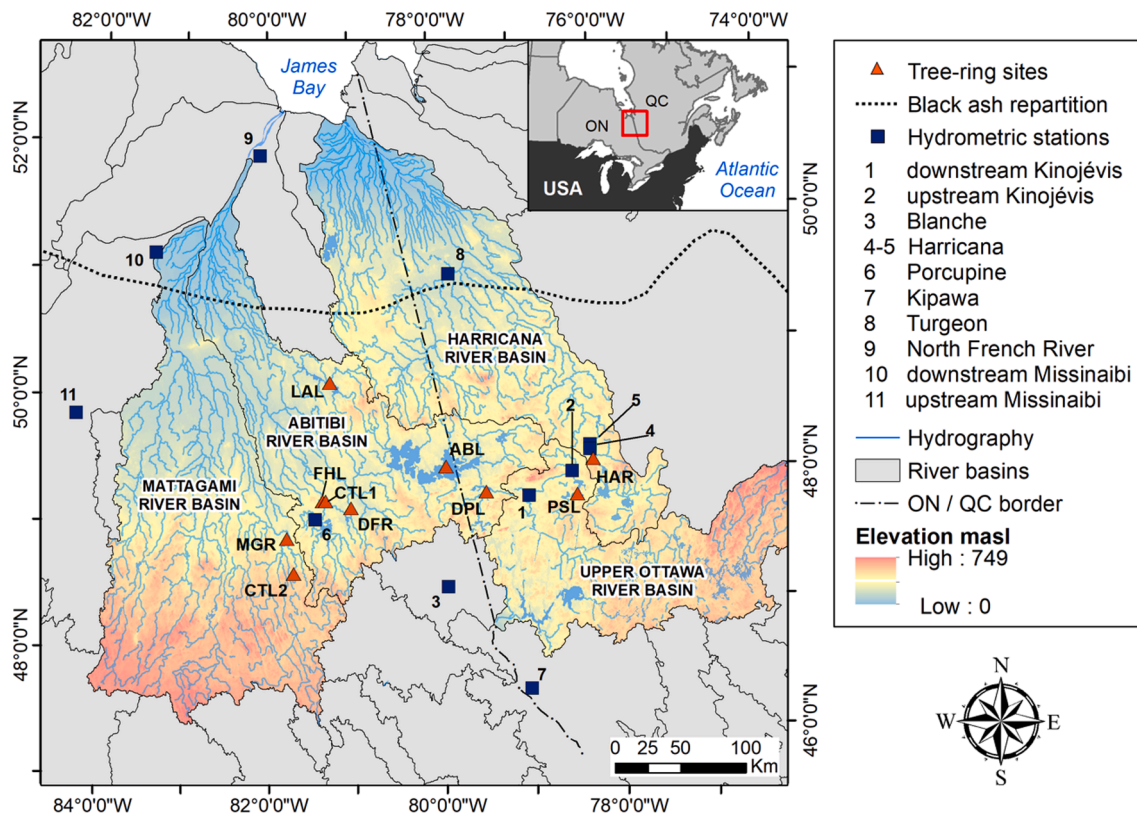


**Fig. 1.** Map of the study area. Location of the study area within North America (upper inset). The tree-ring sampling sites (red triangles) and hydrometric stations (blue squares) are indicated as well as the four major river basins under study. The abbreviations refer to those listed in Table 1, Lake Duparquet is coded ‘DPL’.

*tremuloides* Michx.) (Denneker et al., 1999). Riparian areas are dominated by eastern white cedar (*Thuja occidentalis* L.), and occasionally balsam poplar (*Populus balsamifera* L.) (Tardif and Bergeron, 1992; Denneker et al., 1999). *Fraxinus nigra* can be found in this last associations or it can form pure stands (Tardif and Bergeron, 1997a). For this study, *F. nigra* trees were found in a variety of habitats such as oxbow lakes, sediment bars, meanders, or lake bays where the soil consists of a fine clay deposit and where the topography allows the water table to be accessible most of the year.

2.2. Sampling

Between 2017 and 2018, ten sites distributed along four river basins were sampled including four sites with natural hydrological regime (Lake Duparquet: DPL, Preissac Lake: PSL, Harricana River: HAR and Little Abitibi Lake: LAL); four sites with regulated hydrological regime (Abitibi Lake: ABL, regulated downstream by the Iroquois Falls dam built in 1914; Driftwood River: DFR, regulated downstream by the

Monteith dam built in 1953; Frederick House Lake: FHL, regulated downstream by the Frederick House Lake dam built in 1938; and Mattagami River: MGR, regulated upstream by the Wawaitin Falls dam built in 1912, and downstream by the Sandy Falls dam, built in 1911; Supp. Table 1) and two unflooded control sites in topographically flat upland forests (CTL1, CTL2; Fig. 1, Table 1). Among the regulated river sites, the ABL, DFR and FHL sites are located upstream of the dams while the MGR site is located between two dams. In total, 929 samples were collected from 470 *F. nigra* trees (Table 1). To aid in site selections, aerial photographs and Canada’s National Forest Inventory maps (<https://nfi.nfis.org>) coupled with SRTM elevation data (<https://earthexplorer.usgs.gov/>) were used. The Québec (CEHQ, 2019) and Ontario dam inventories (OMNRF, 2019) were used to characterize each sampling site according to hydrological regimes (presence of a dam and its distance to the sampling site). Increment cores were taken from living trees and stem discs were collected from dead trees with all samples collected as close to the ground level as possible. Wood samples were prepared and sanded following standard dendrochronological procedures (Phipps,

**Table 1**

Number of *Fraxinus nigra* trees sampled, and cores collected per site. Sites are classified by hydrological regime. The field ‘‘Period’’ indicates the maximum period covered by the flood-ring and continuous series of earlywood vessel chronologies. The distance provided are in reference to Lake Duparquet’s location. Among the regulated river sites, the ABL, DFR and FHL sites are located upstream of the dams while the MGR site is located between two dams.

Discharge	Code	Distance (km)	Site	River Basin	Trees	Samples	Period
Natural	DPL	/	Duparquet Lake	Abitibi	65	123	1750–2016
	PSL	70	Preissac Lake	Upper Ottawa	37	74	1812–2016
	HAR	85	Harricana River	Harricana	120	239	1780–2016
	LAL	145	Little Abitibi Lake	Abitibi	48	96	1793–2016
Regulated	ABL	30	Abitibi Lake	Abitibi	12	24	1901–2016
	DFR	105	Driftwood River	Abitibi	43	86	1852–2016
	FHL	125	Frederick House Lake	Abitibi	67	132	1774–2016
	MGR	150	Mattagami River	Mattagami	32	64	1904–2016
Control	CTL1	120	Frederick House Lake	Abitibi	24	47	1904–2016
	CTL2	160	Bruce Lake	Mattagami	22	44	1755–2016



1985; Cook and Kairiukstis, 1990). Prior to visual identification of flood rings, the prepared sample wood surfaces were rubbed with white chalk to increase the contrast between earlywood vessels and other cell types (St. George et al., 2002; Tardif and Conciatori, 2006b).

### 2.3. Tree-ring data

Each sample was systematically inspected with a dissecting microscope to visually determine the presence of flood ring and their presence was labelled on the core mount prior to visual crossdating. Flood rings were categorized into two classes in relation to their vessel size, vessel density and organization within the earlywood (Fig. 2). This visual identification step was carried out by two observers, who each had half of the samples amount. A dual numerical code was used, with a F1 indicating a weakly defined flood ring (noticeable increase in number of earlywood vessels supported with a decrease in earlywood vessel area) and a F2 indicating a well-defined flood ring as previously described in *F. nigra* (Tardif et al., 2010; Kames et al., 2016; Nolin et al., 2021; Fig. 2). This characterisation of flood rings (F1 or F2) was chosen to account for the intensity of flood rings rather than a simple presence-absence index. Given that tree elevation and coring height varied within a site and that anatomical changes in earlywood vessels (flood ring) were reported to occur solely in the submerged portion of the tree stem during active earlywood formation (St. George et al., 2002; Copini et al., 2016), adopting a dual numerical code aimed to better capture the flood signal. After flood-ring identification on each sample was completed, visual crossdating was performed using *F. nigra* pointed years developed for Lake Duparquet (Tardif and Bergeron, 1997a; Kames et al., 2016; Nolin et al., 2021) and the list method (Phipps, 1985).

In addition to flood-ring identifications, annual measurements of tree-ring earlywood vessels were performed on a small subset of trees. The mean cross-sectional lumen area (MVA) and the number of earlywood vessels (N) were measured in six *F. nigra* samples. These samples were selected to be the oldest and best-preserved wood samples (e.g., clear tree rings, no rot, etc.) from the four river basins and corresponded to natural and regulated hydrological regimes: Abitibi River basin (natural, site LAL, n=2); Harricana River basin (natural, site HAR, n=2); upper Ottawa River basin (natural, site PSL, n=1); Mattagami River basin (regulated, site MGR, n=1; Fig. 1; Table 1). The MVA and N chronologies previously developed for Lake Duparquet (1771-2016, n=43) by Nolin et al. (2021) were used as references.

Measurement of mean cross-sectional area (MVA) and number (N) of earlywood vessel in annually resolved tree rings was performed as described in Nolin et al. (2021) using high-resolution scanned images of the tree rings. The images were acquired from a Nikon DS-Fi1 camera

mounted on a NIKON SMZ1000 stereomicroscope to produce standardized tree-ring images format (1600 × 1200 dpi at ×20 magnification). Earlywood vessels were automatically detected and digitalized using the Canny edge algorithm (Canny, 1986) implemented in ImageJ2X software (Rueden et al., 2017). Each earlywood vessel shape was checked and false automatic delimitations (e.g., incomplete earlywood vessel lumen areas at the edge of the cores, grouped earlywood vessels, tyloses) were manually corrected with a graphic tablet. After ensuring that each earlywood vessel contour delineation was correct, the measurements of annual MVA and N were performed using WinCell software Pro v2018c (Régent Instrument, 2018). Both MVA and N were measured on earlywood vessel areas greater than 3000 μm<sup>2</sup> in cross-section (Tardif, unpublished data). The delimitation between earlywood and latewood has been qualitatively identified as the abrupt decrease in vessel cross-sectional area (Tardif and Conciatori, 2006b; Kames et al., 2016).

Series crossdating and measurements were validated with CDendro (Larsson, 2003) and COFECHA (Holmes, 1983) prior to series' detrending. Each tree-ring series was divided by a cubic smoothing spline function with 50% frequency of response of 60 years (Cook and Kairiukstis, 1990). Six missing values have been interpolated by the Spline filling function of the 'dplR' package to detrend the series (Bunn, 2008). Detrended series were then combined into standardized chronologies per river basins and hydrological regimes using a bi-weight robust mean (when n > 1 series) to lower the influence of outliers. This was the case for the Abitibi and the Harricana rivers (n = 2 series). All statistical procedures of dendrochronology were conducted with the 'dplR' package (Bunn, 2008) in R environment (R Core Team, 2020).

### 2.4. Hydrological data

Daily discharges were downloaded from the Water Survey of Canada, the Reference Hydrometric Basin Network and the Centre d'Expertise Hydrique du Québec (Supp. Table 2). Eleven hydrometric stations were selected on natural rivers not regulated by dams (Supp. Table 2) and with a minimum of 24 years of data, but not necessarily in a continuous sequence. Daily discharges were averaged from April 15 to June 30. This period best represented the range of discharge variability during the spring flood season and can be equated with the period of earlywood formation in *F. nigra* (Nolin et al., 2021). Only years with less than 10 % missing daily values for the period 15 April to 30 June (77 days) were considered. This arbitrary threshold was chosen to avoid statistical shortcomings in the interpolation of missing values. It should be noted that the data for Harricana River came from two hydrometric stations in close proximity (4 km) and for the same drainage area. They have

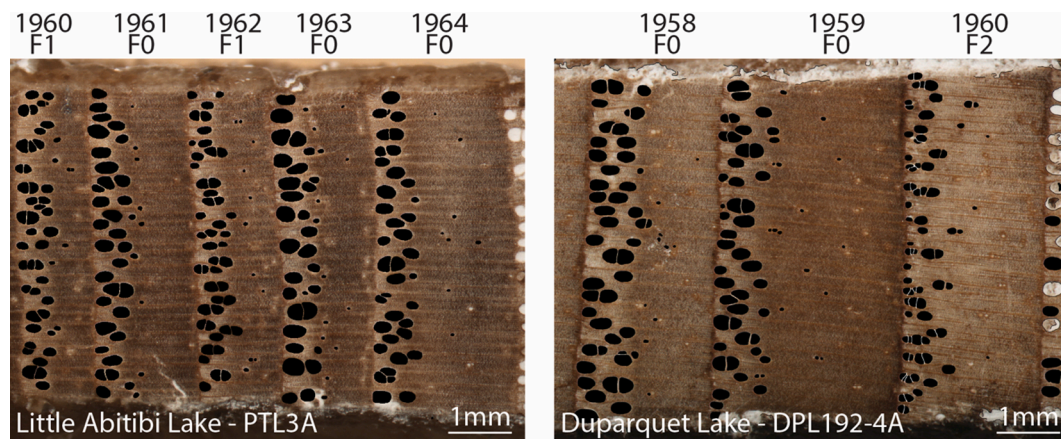


Fig. 2. Segmented earlywood vessels in *Fraxinus nigra* tree rings. Vessels appear black as the result of the digitalization process. The years are given with the classification of flood rings: F0 = null, F1 = weakly defined flood ring and F2 = well-defined flood ring. Notice the difference in the strength of the flood rings between Little Abitibi Lake (left) and Lake Duparquet (right) for the year 1960.

therefore been grouped into a single time series because they overlap with no difference in daily discharge values (Kames et al., 2016; Nolin et al., 2021). In addition to these hydrometric records, the Harricana River spring discharge reconstruction from Nolin et al. (2021) was used for comparison.

## 2.5. Statistical analyses

The spatial coherency of flood rings among the four river basins and Lake Duparquet was assessed using four approaches. First, annual flood-ring series were compiled by tree, keeping for each year the code that had the maximum intensity between the two radii ( $0 < F1 < F2$ ). Spearman's rank correlation coefficients were calculated between each flood-ring series per tree (categorical variable: value = 0, 1 or 2) and the reconstructed Harricana River spring discharge (continuous variable) over the maximum series length (n ranging from 113 to 246 years). The dispersion of correlation coefficients between sites, and between hydrological regimes were compared using box plots (Legendre and Legendre, 2012). When flood-ring series were compared to the reconstruction of the Harricana River spring discharge, which is derived from *F. nigra* trees growing on the floodplain of Lake Duparquet, the dispersion of correlation coefficients between sites was compared by geographic distance to Lake Duparquet.

Second, flood-ring series per tree were used to calculate, for each of the ten sampled sites, three flood-ring relative frequencies F1, F2 and

F12 (hereafter flood-ring chronologies). F1 and F2 can be defined as the annual sum of flood rings for a given year, divided by the annual sum of samples for the same year and expressed as the percentage of F1 and F2 rings over the total number of samples in a given year. F12 is the sum of F1 + F2 chronologies and was used to determine whether or not the F1 and F2 flood-ring classes carry different hydrological signal. Each flood-ring chronology (F1, F2, F12) was correlated using Spearman's rank correlation coefficient i) with the reconstructed spring discharge of the Harricana River, ii) with spring discharge records from 11 hydrometric stations, iii) among river basins, iv) and among hydrological regimes.

Third, and in the same way, earlywood vessel chronologies (MVA and N) were correlated using Pearson's correlation coefficient i) with the reconstructed spring discharge of the Harricana River (Nolin et al., 2021), ii) with spring discharge records from 11 hydrometric stations, iii) among river basins, and iv) and among hydrological regimes. At last, the periodicities that dominate the variance through time were compared using continuous wavelet transform (CWT) on the mean standardized earlywood vessel chronologies (MVA and N) from the four river basins. CWT were computed on a  $\omega_0 = 6$  Morlet power spectrum base so the Morlet wavelet scale be comparable to the Fourier period (Torrence and Compo, 1998). Significant peaks in spectra were tested against a white-noise background on 1,000 Monte Carlo iterations (Torrence and Compo, 1998). All analyses were conducted using R software (R Core Team, 2020) and the packages 'Hmisc' (Harrell, 2020) for correlations analyses, and 'biwavelet' (Gouhier et al., 2019) for

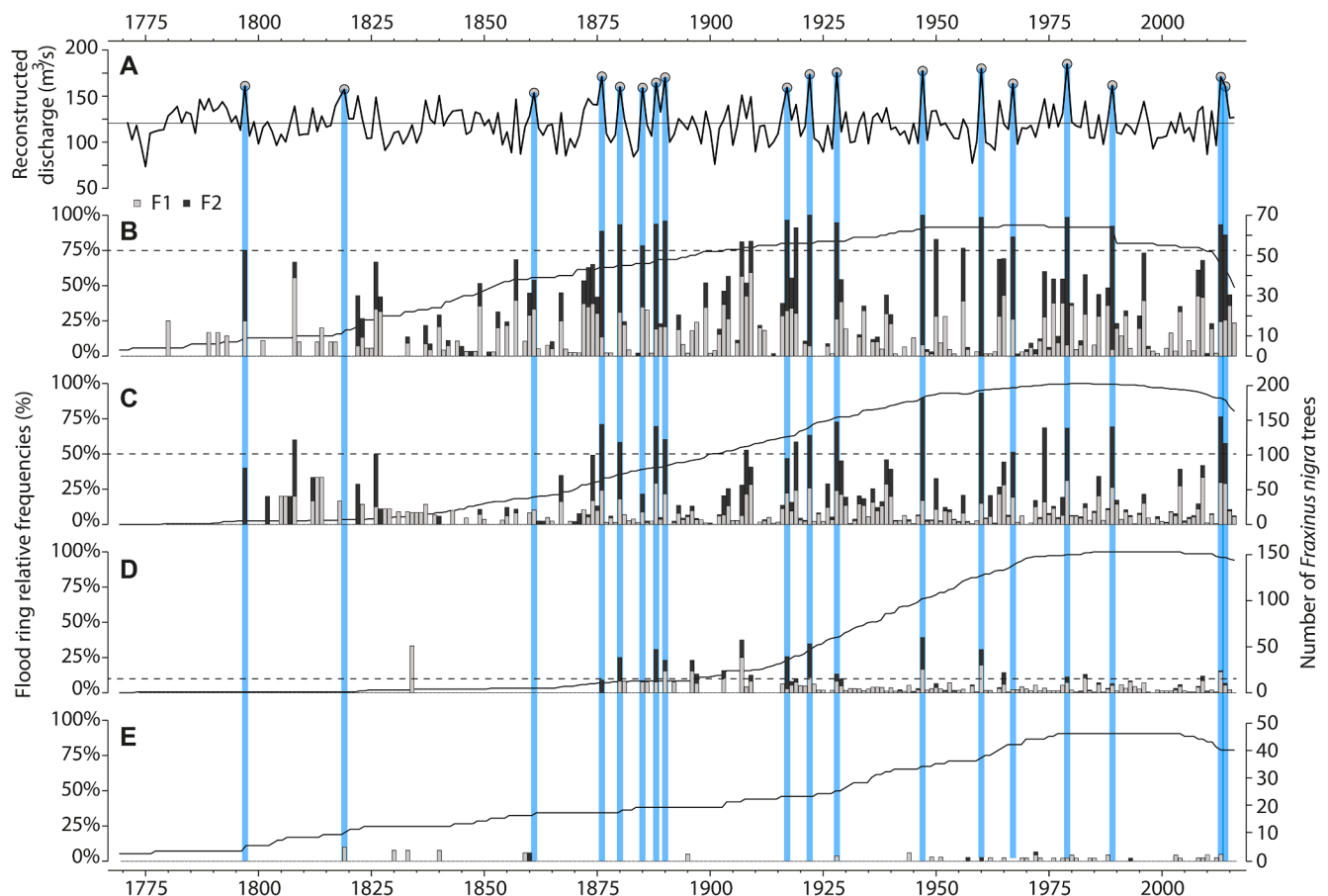


**Fig. 3.** Flood-ring chronologies among hydrological regimes. Comparison between (A) the reconstructed Harricana River discharge flood-ring relative chronologies from *Fraxinus nigra* trees from (B) Lake Duparquet (DPL), (C) pooled natural rivers (PSL, HAR, LAL), (D) regulated rivers (ABL, DFR, FHL, MGR), and (E) unflooded control sites (CTL1, CTL2). Grey and black histograms are respectively F1 and F2 flood-ring relative frequencies. The background solid black lines indicate the number of trees per year. The dashed horizontal lines indicate the three thresholds used to extract the highest F12 values from the three hydrological regimes, and respectively  $F12 \geq 75\%$  for Lake Duparquet,  $F12 \geq 50\%$  for natural rivers and  $F12 \geq 10\%$  for regulated rivers. The 18 years with the highest reconstructed spring discharge for the Harricana River and over the last 250 years are represented by grey dots on the upper A curve and extending as blue bars. Those 18 years were defined using a threshold corresponding to the mean + 1.5 SD (threshold value =  $151.3 \text{ m}^3/\text{s}$ ; Nolin et al., 2021).

continuous wavelet transformations.

### 3. Results

#### 3.1. Flood ring coherency across river basins

The flood-ring chronologies covered the period 1770–2016 with one tree per river basin going back to 1770 (Fig. 3). The sample replication indicated that trees sampled from the four regulated rivers (ABL, DFR, FHL, MGR) were generally younger than in other hydrological regimes with few trees available before the 1850's (n=4). The F1 and F2 chronologies (Fig. 3) were highly intercorrelated over the common period 1780–2016 on Lake Duparquet ( $\rho = 0.68$ ,  $p < 0.001$ ), natural rivers ( $\rho = 0.59$ ,  $p < 0.001$ ) and regulated rivers ( $\rho = 0.55$ ,  $p < 0.001$ ), but not on unflooded control sites ( $\rho = 0.03$ ,  $p = 0.606$ ). The F12 chronologies were more strongly correlated to instrumental and reconstructed spring discharge than either the F1 or F2 chronologies (Table 3). The F12 chronologies for both Lake Duparquet (maximum value of 100%) and natural rivers (maximum value of 93.3%) demonstrated a higher proportion of flood rings than for regulated rivers (maximum value of 39.2%) and unflooded control sites (maximum value of 10.0%; Fig. 3). Indeed, each correlation between flood-ring chronologies and the different datasets used in this study were highest for Lake Duparquet, higher in natural rivers than in regulated rivers, and centered around zero for the unflooded control sites (Figs. 3, 4, Tables 2, 3). In the spatial structure of correlations, associations between each flood-ring chronologies and instrumental spring discharge records tended to weaken with increasing distance to Lake Duparquet and in regulated rivers (Fig. 4, Table 3); the lowest number of significant associations being found with the southernmost hydrometric station of Kipawa River (Table 3).

Flood-ring chronology values (F12) were compared to the reconstructed spring discharge of the Harricana River for the period 1771–2016 (Fig. 3). Nolin et al. (2021) estimated using the reconstruction mean value + 1.5 standard deviation ( $151.3 \text{ m}^3/\text{s}$ ) that the most severe spring flood years had occurred in 1797, 1819, 1861, 1876, 1880, 1885, 1888, 1890, 1917, 1922, 1928, 1947, 1960, 1967, 1979, 1989, 2013 and 2014 (Fig. 3A). Given the variation in hydrological regimes and the number of sampled trees within each, an arbitrary threshold was determined to extract the highest F12 values from each regime. These thresholds were respectively  $F12 \geq 75\%$  for Lake Duparquet,  $F12 \geq 50\%$  for natural rivers and  $F12 \geq 10\%$  for regulated rivers (Fig. 3). According to these three thresholds, the highest values in the F12 flood-ring chronologies corresponded well with the 18 years of highest reconstructed discharge years since 1771 with respectively 16/18, 14/18 and 10/18 years captured for Lake Duparquet, natural rivers and regulated rivers.

In each of the hydrological regimes, some years with high F12 values (above the pre-determined thresholds) did not match with the 18 most severe spring floods identified using the reconstructed spring discharge

of the Harricana River (Fig. 3; and Supp. Table 3). For the most part these years were, however, very close to the  $151.3 \text{ m}^3/\text{s}$  threshold used to estimate the most severe spring floods (Supp. Table 3). For Lake Duparquet, the five mismatched F12 years with values  $\geq 75\%$  (1907, 1909, 1919, 1950 and 1956) corresponded to reconstructed discharges between  $125.0$  and  $151.1 \text{ m}^3/\text{s}$ . Similarly, the five F12 year with values  $\geq 50\%$  for the natural rivers 1808, 1826, 1908, 1919 and 1974) corresponded to reconstructed discharges between  $125.7$  and  $148.8 \text{ m}^3/\text{s}$ . For the regulated rivers, ten F12 values  $\geq 10\%$  also corresponded to reconstructed discharge ranging from  $116.2$  to  $151.1 \text{ m}^3/\text{s}$ .

Ten high F12 values in regulated rivers chronology were also not indicated by equivalent high F12 values in natural rivers, Lake Duparquet, or in the reconstructed spring discharge of the Harricana River (Fig. 3). The F12 chronologies from regulated rivers never reached more than 40% with a marked decrease in F2 flood-ring frequency observed after ca. 1920 (Fig. 3D). Looking at the individual regulated sites averaged to produce the regulated flood-ring chronologies revealed that both lake sites (ABL and FHL) recorded very little flood rings compared to the two river sites (DFR and MGR; results not shown). These differences in flood-ring chronologies (F1, F2, F12) were further emphasized by the regulated Driftwood River (DFR; 1852–2016) and Mattagami River (MGR; 1904–2016) being significantly correlated with the reconstructed Harricana River spring discharge and not the Abitibi Lake and Frederick House Lake (ABL, FHL; Table 2). Before the 1920s the chronologies presented few flood rings, and after the 1920s flood rings matched the highest spring discharge years reconstructed for the Harricana River.

In the unflooded control sites, the flood rings observed were mostly F1 and were never present in more than 10% of the trees (Fig. 3E). Flood-rings series per tree and flood-ring chronologies in the unflooded control sites showed no significant association with the reconstructed Harricana River spring discharge (Table 2; Fig. 4) or with the 11 hydrometric records (Table 3). Two values corresponded to the highest 18 spring discharge years reconstructed in the Harricana River (1819: 10%, 1 tree out of 10; 2013: 4.87%, 2 trees out of 41).

#### 3.2. Continuous earlywood vessel chronologies

Continuous chronologies of earlywood vessels spanned different time periods for Lake Duparquet (1771–2016) and for the four river basins (Harricana: 1783–2016; upper Ottawa: 1814–2016; Abitibi: 1840–2016; and Mattagami: 1922–2016; Fig. 5 left panels).

Inter-series correlations were high in chronologies produced from two tree series. For example, in MVA chronologies from Harricana and Abitibi River,  $r = 0.73$  ( $n = 129$ ,  $p < 0.001$ ) and  $r = 0.68$  ( $n = 119$ ,  $p < 0.001$ ; Fig. 5). Correlations between earlywood vessel and F12 chronologies were high in Lake Duparquet (respectively for MVA and N,  $\rho = -0.73$  and  $0.54$ ,  $p < 0.001$ , 1771–2016) and natural rivers ( $\rho = -0.53$  and  $0.43$ ,  $p < 0.001$ , 1783–2016). In regulated rivers, correlations were weaker (MVA:  $r = 0.29$ ,  $p = 0.0042$ , 1922–2016; N:  $r = -0.14$ ,  $p = 0.1856$ , 1922–2016). Generally, the amplitude of interannual variability

**Table 2**

Spearman's rank correlation coefficients ( $\rho$ ) and p values (p) between the flood-ring chronologies at each site and the reconstructed Harricana River spring discharge. F1 and F2 represent weakly and well-defined flood rings and F12 is the sum of their relative frequencies. Bold characters denote p values  $< 0.05$ .

Discharge	Sites	Period	N years	F1		F2		F12	
				$\rho$	p	$\rho$	p	$\rho$	p
Natural	DPL	1771–2016	246	<b>0.57</b>	0.0000	<b>0.63</b>	0.0000	<b>0.66</b>	0.0000
	PSL	1812–2016	205	<b>0.44</b>	0.0000	<b>0.40</b>	0.0000	<b>0.43</b>	0.0000
	HAR	1780–2016	237	<b>0.36</b>	0.0000	<b>0.48</b>	0.0000	<b>0.44</b>	0.0000
	LAL	1793–2016	224	<b>0.35</b>	0.0000	<b>0.46</b>	0.0000	<b>0.44</b>	0.0000
Regulated	ABL	1901–2016	116	0.13	0.1806	0.10	0.2628	0.15	0.1057
	DFR	1852–2016	165	<b>0.36</b>	0.0000	<b>0.46</b>	0.0000	<b>0.43</b>	0.0000
	FHL	1774–2016	243	0.05	0.4316	<b>0.21</b>	0.0013	0.07	0.2670
	MGR	1904–2016	113	<b>0.29</b>	0.0015	<b>0.22</b>	0.0174	<b>0.30</b>	0.0015
Control	CTL1	1904–2016	113	0.09	0.3501	0.05	0.6313	0.12	0.1955
	CTL2	1771–2016	246	-0.04	0.5740	0.02	0.7632	-0.02	0.6967



**Table 3**

Spearman's rank correlation coefficients ( $\rho$ ) and p-values (p) between flood-ring chronologies from Lake Duparquet (DPL), natural rivers (NAT), regulated rivers (REG) and unflooded control sites (CTL) and 10 instrumental records of April 15 to June 30 mean discharge across the study area. The field "Id" is the Canadian federal hydrometric station identification number. F1 and F2 represent weakly and well-defined flood rings and F12 is the sum of the relative frequencies F1 and F2. The table is ordered by increasing distance between hydrometric station and Lake Duparquet (left to right) to visualize spatial coherency in the correlation structure. Bold characters denote p values < 0.05.

Station	Kinojévis River	Kinojévis River	Blanche River	Harricana River	Porcupine River	Kipawa River	Turgeon River	Missinaibi River	North French River	Missinaibi River
Id	02JB013	02JB003	02JC008	04NA001-2	04MD004	02JE015	04NB001	04LM001	04MF001	04LJ001
Period	1971–2016	1938–1965	1970–2016	1915–2016	1977–2015	1963–2011	1969–1999	1973–2016	1967–2016	1921–2016
N years	46	28	47	102	26	38	24	43	50	96
Distance (km)	30	70	80	85	130	155	170	310	310	320
DPLF1	$\rho$ <b>0.61</b>	<b>0.51</b>	<b>0.54</b>	<b>0.57</b>	<b>0.52</b>	<b>0.40</b>	<b>0.60</b>	<b>0.52</b>	<b>0.57</b>	<b>0.29</b>
	p 0.0000	0.0056	0.0001	0.0000	0.0063	0.0119	0.0018	0.0004	0.0000	0.0045
DPLF2	$\rho$ <b>0.77</b>	<b>0.61</b>	<b>0.58</b>	<b>0.66</b>	<b>0.70</b>	<b>0.35</b>	<b>0.64</b>	<b>0.59</b>	<b>0.37</b>	<b>0.36</b>
	p 0.0000	0.0005	0.0000	0.0000	0.0001	0.0307	0.0007	0.0000	0.0085	0.0003
DPLF12	$\rho$ <b>0.80</b>	<b>0.74</b>	<b>0.68</b>	<b>0.73</b>	<b>0.78</b>	<b>0.48</b>	<b>0.75</b>	<b>0.64</b>	<b>0.55</b>	<b>0.42</b>
	p 0.0000	0.0000	0.0000	0.0000	0.0000	0.0023	0.0000	0.0000	0.0000	0.0000
NATF1	$\rho$ <b>0.76</b>	<b>0.66</b>	<b>0.67</b>	<b>0.75</b>	<b>0.77</b>	<b>0.34</b>	<b>0.77</b>	<b>0.71</b>	<b>0.57</b>	<b>0.54</b>
	p 0.0000	0.0001	0.0000	0.0000	0.0000	0.0349	0.0000	0.0000	0.0000	0.0000
NATF2	$\rho$ <b>0.60</b>	<b>0.49</b>	<b>0.60</b>	<b>0.61</b>	<b>0.76</b>	0.26	<b>0.63</b>	<b>0.61</b>	<b>0.53</b>	<b>0.47</b>
	p 0.0000	0.0076	0.0000	0.0000	0.0000	0.1107	0.0009	0.0000	0.0001	0.0000
NATF12	$\rho$ <b>0.75</b>	<b>0.62</b>	<b>0.63</b>	<b>0.73</b>	<b>0.78</b>	<b>0.34</b>	<b>0.79</b>	<b>0.73</b>	<b>0.58</b>	<b>0.54</b>
	p 0.0000	0.0004	0.0000	0.0000	0.0000	0.0347	0.0000	0.0000	0.0000	0.0000
REGF1	$\rho$ <b>0.54</b>	0.19	<b>0.41</b>	<b>0.39</b>	<b>0.65</b>	0.28	<b>0.54</b>	<b>0.56</b>	<b>0.30</b>	<b>0.36</b>
	p 0.0001	0.3299	0.0045	0.0000	0.0004	0.0871	0.0068	0.0001	0.0327	0.0003
REGF2	$\rho$ <b>0.42</b>	<b>0.45</b>	<b>0.38</b>	<b>0.36</b>	<b>0.54</b>	-0.14	0.34	<b>0.37</b>	0.25	0.19
	p 0.0038	0.0160	0.0081	0.0002	0.0044	0.4002	0.1045	0.0149	0.0817	0.0682
REGF12	$\rho$ <b>0.56</b>	0.27	<b>0.41</b>	<b>0.42</b>	<b>0.67</b>	0.23	<b>0.56</b>	<b>0.56</b>	<b>0.29</b>	<b>0.36</b>
	p 0.0001	0.1587	0.0042	0.0000	0.0002	0.1722	0.0047	0.0001	0.0390	0.0003
CTLF1	$\rho$ -0.04	0.02	0.05	0.04	0.09	0.07	0.10	0.07	0.03	-0.03
	p 0.7732	0.9143	0.7513	0.7211	0.6630	0.6888	0.6578	0.6222	0.8227	0.7973
CTLF2	$\rho$ -0.17	0.14	-0.12	-0.06	0.12	-0.06	-0.22	0.06	-0.04	0.11
	p 0.2648	0.4667	0.4373	0.5359	0.5593	0.7322	0.2969	0.6921	0.8014	0.2995
CTLF12	$\rho$ -0.08	0.10	0.03	0.03	0.12	0.02	0.07	0.08	0.03	0.02
	p 0.6078	0.6203	0.8645	0.8018	0.5533	0.9180	0.7318	0.6094	0.8245	0.8318

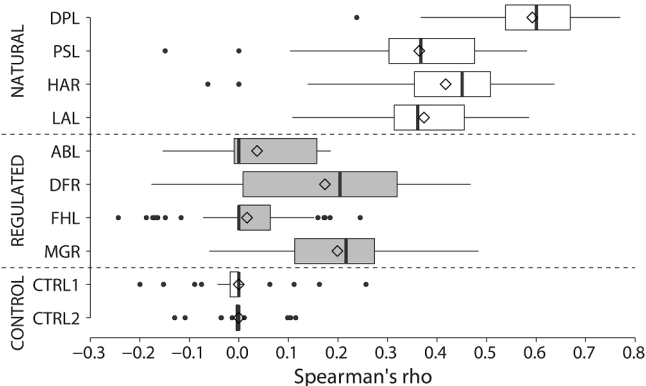


**Fig. 4.** Box plot of the dispersion of Spearman's rank correlation coefficients between flood-ring series per tree and the reconstruction of the Harricana River spring discharge. Correlations are pooled by river hydrological regime (natural, regulated and unflooded control; separated by dotted lines and respectively from top to bottom) and by increasing distance from sites to Lake Duparquet. Site abbreviations are defined in Table 1. The left and right-most edges of the rectangles indicate the interquartile range between the 25<sup>th</sup> and 75<sup>th</sup> percentiles and the dots indicate outliers outside the 10<sup>th</sup> and 90<sup>th</sup> percentiles. The center line of the graph indicates the median, and the diamond indicates the mean.

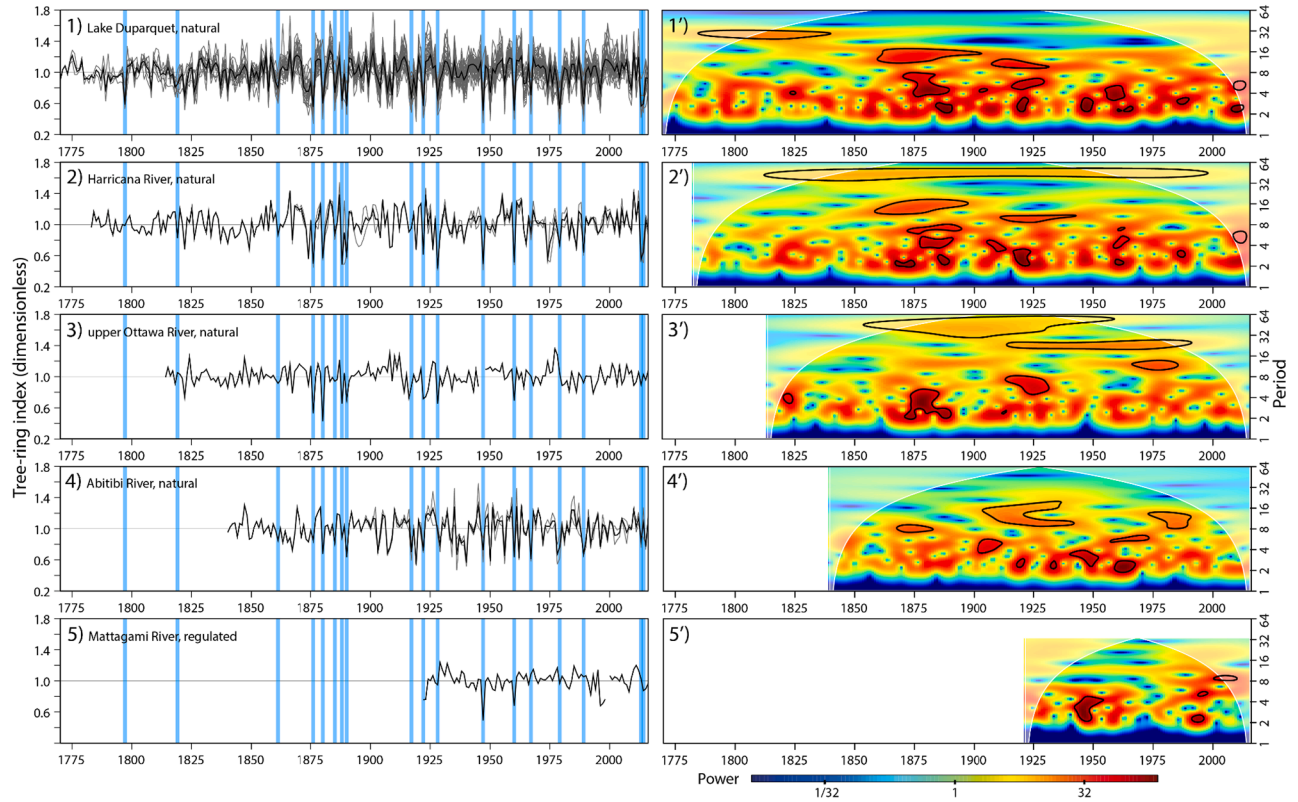
was higher in MVA than in N chronologies (Fig. 5) and these two variables were negatively intercorrelated (Lake Duparquet:  $r = -0.65$ ,  $p < 0.001$ ,  $n = 244$ ; Harricana:  $r = -0.47$ ,  $p < 0.001$ ,  $n = 232$ ; upper Ottawa:  $r = -0.41$ ,  $p < 0.001$ ,  $n = 199$ ; Abitibi:  $r = -0.58$ ,  $p < 0.001$ ,  $n = 175$ ; and Mattagami River:  $r = -0.28$ ,  $p < 0.05$ ,  $n = 92$ ). The highest spring discharge years reconstructed for the Harricana River were well captured by MVA and N chronologies from Lake Duparquet, and natural

ivers. Each of those chronologies showed 1947 and 1960 as the highest spring discharge magnitude in the last 250 years and the years 1880, 1890, 1922, 1989, 2013, and 2014 also shared particularly high values (Fig. 5).

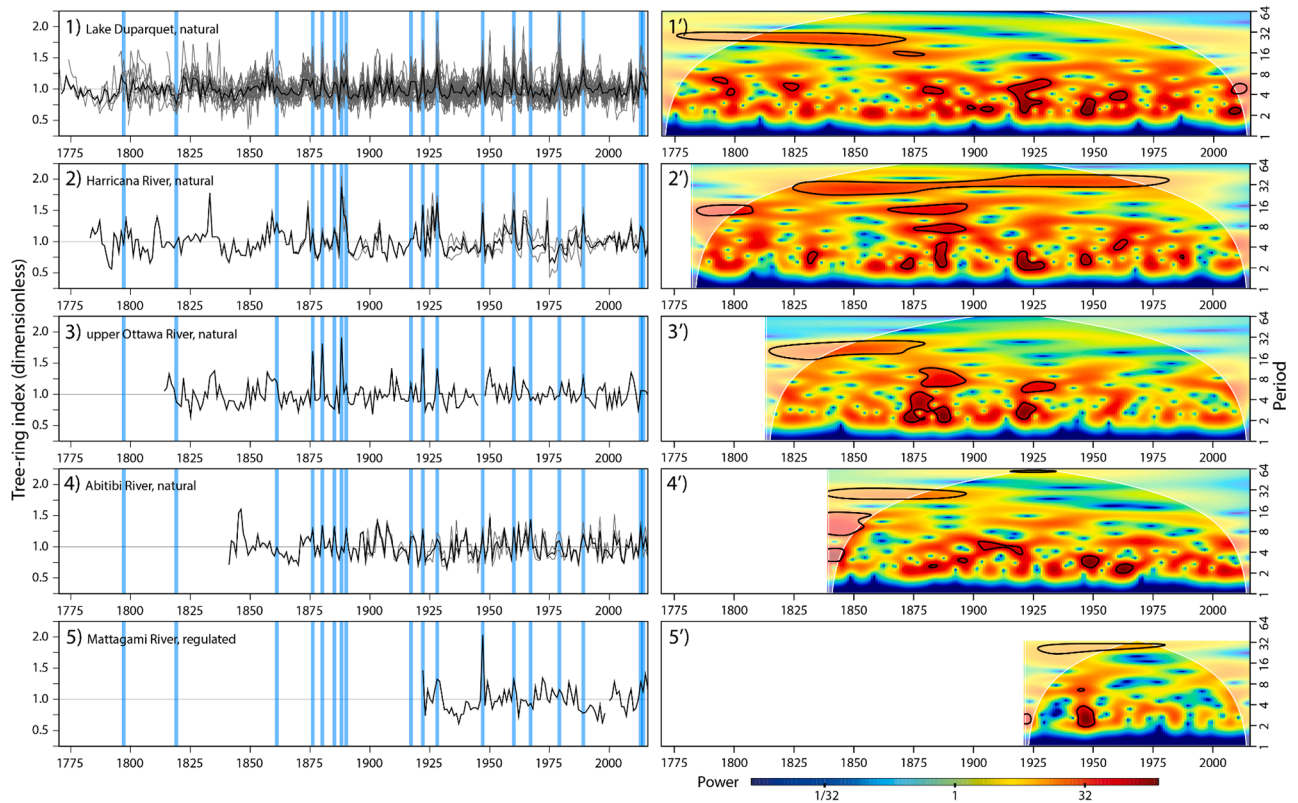
Correlations of earlywood vessel chronologies among river basins and hydrological regimes (Table 4) and with hydrometric records (Table 5; Fig. 1) were highly significant. As with flood-ring chronologies, associations with earlywood vessel chronologies were found to be highest with Lake Duparquet, higher among natural rivers than for regulated rivers and to weaken with increasing distance from Lake Duparquet (Tables 4, 5). The lowest correlations were found between the MVA and N chronologies from the upper Ottawa River and the southernmost hydrometric record of Kipawa River, both flowing South to the Saint-Lawrence River (Tables 4, 5). Compared to the N chronologies, the MVA chronologies were less associated among river basins and showed a greater number of significant correlations (10/10 vs 4/10 for MVA; Table 4). In the structure of correlations between earlywood vessel chronologies and hydrometric records, the opposite was observed. The associations between MVA and hydrometric records were about twice as high as with N and showed a greater number of significant associations (Table 5).

Continuous wavelet transformation allowed to investigate the temporal coherency of the earlywood vessel chronologies from the different hydrological regimes ( $n = 1$  or  $n = 2$  trees) to the more robust Lake Duparquet MVA and N chronologies ( $n = 43$  trees). Since the MVA and N chronologies were significantly correlated with the regional spring discharge records, it can be hypothesized that the decomposition of their periodicities may reflect the decomposition of periodicities affecting regional spring discharge. Three major patterns of significant high variance were observed in the power spectrum of chronologies from natural regimes (Fig. 5 right panels). A first pattern of 32-year significant periodicity was persistent in MVA and N chronologies from Lake

A) Mean earlywood vessel area (MVA)



B) Number of earlywood vessels (N)



(caption on next page)



**Fig. 5.** Comparison between continuous earlywood vessel chronologies and their continuous wavelet transform among river basins. A) Chronologies of mean earlywood vessel cross-sectional area (MVA). B) Chronologies of number of earlywood vessels (N). Left panel is the comparison between chronologies from Lake Duparquet and from the four river basins. The vertical blue bars indicate the 18 years with the highest reconstructed spring discharge for the Harricana River and over the last 250 years. Those 18 years were defined using a threshold corresponding to the mean + 1.5 SD (threshold value = 151.3 m<sup>3</sup>/s; Nolin et al., 2021). Right panel is the decomposition of mean standardized chronologies into Morlet 6<sup>th</sup> power in continuous wavelet transform. The color bar gives the range of variance intensity from low (blue) to high (red) and black lines encircle significant high variance tested against a white noise background at a p-value < 0.05. The cone of influence is figured in white and delimit areas where wavelets are altered by edge-effect. For both A) and B) right and left panels, chronologies are as follow: 1) Lake Duparquet, 1771-2016, n = 43; 2) Harricana River basin, site HAR, 1783-2016, n = 2; 3) upper Ottawa River basin, site PSL, 1814-2016, n = 1; 4) Abitibi River, site LAL, 1840-2016, n = 2 and 5) Mattagami River, site MGR, 1922-2016, n = 1. The Lake Duparquet, Harricana, Abitibi and upper Ottawa River chronologies were developed from trees growing with natural discharge, while the Mattagami River basin index is from a site where the river is regulated by a dam.

**Table 4**

Pearson's correlations (r) and p values (p) between continuous earlywood vessels chronologies from the naturally flowing Lake Duparquet (n=43), Harricana River (site HAR, n=2), Abitibi River (site LAL, n=2), upper Ottawa River (site PSL, n=1) and the regulated Mattagami River (site MGR, n=1). Chronologies abbreviation are as follows: (MVA) mean cross-sectional lumen area of earlywood vessels, (N) number of earlywood vessels. Pearson's correlation coefficients are given for the common period 1922-2016 and bold characters denote p values < 0.05.

Sites/Chronologies		MVA	N
Duparquet/Harricana	r	<b>0.81</b>	<b>0.71</b>
	p	0.0000	0.0000
Duparquet/Abitibi	r	<b>0.61</b>	<b>0.59</b>
	p	0.0000	0.0000
Duparquet/upper Ottawa	r	0.20	<b>0.51</b>
	p	0.0551	0.0000
Duparquet/Mattagami	r	<b>0.31</b>	<b>0.50</b>
	p	0.0025	0.0000
Harricana/Abitibi	r	<b>0.41</b>	<b>0.41</b>
	p	0.0000	0.0000
Harricana/upper Ottawa	r	0.15	<b>0.40</b>
	p	0.1408	0.0000
Harricana/Mattagami	r	0.19	<b>0.43</b>
	p	0.0594	0.0000
Abitibi/upper Ottawa	r	0.17	<b>0.37</b>
	p	0.0999	0.0003
Abitibi/Mattagami	r	0.19	<b>0.35</b>
	p	0.0657	0.0004
Mattagami/upper Ottawa	r	0.15	<b>0.28</b>
	p	0.1595	0.0066

Duparquet up to ~1850 and persisted from ~1800 to 1975 in the Harricana River chronologies. In the upper Ottawa River chronologies, only the MVA showed a significant 32-year periodicity affecting the variance from ~1850 to 1950. A second pattern near a 16-year periodicity was more variable over time and between river basins than the 32-year pattern. It started around 1850 in Lake Duparquet and around 1900 in other chronologies from natural rivers. A third pattern was the apparition of decadal periodicities of 8-years and less from ~1875 and 1900 in chronologies from natural rivers except the upper Ottawa River. The chronologies from the regulated Mattagami River began in 1922 and were not long enough to support the accurate calculation of high periodicities (low frequencies). However, the N chronology showed significant high variance similar to that found in natural rivers chronologies. Notably, around a decadal periodicity in 1940 and around a 32-year periodicity from 1925 to 1980, although outside the cone of influence.

## 4. Discussion

### 4.1. Spatial coherency among spring flood proxy from natural rivers

In this study, results showed that both flood-ring chronologies (F1, F2, F12) and earlywood tree-ring anatomical chronologies (MVA and N), hereafter referred to as spring flood proxies, were highly intercorrelated. Spring flood proxies were strongly correlated to Harricana River spring discharge and to instrumental data from eleven hydrometric records

distributed across a wide boreal territory (above 70 000 km<sup>2</sup>). Spring flood proxies provided synchronous evidence of flooding across the four river basins with most of the major spring floods reconstructed for the Harricana River for the last 250 years being recorded by *F. nigra* trees growing along Lake Duparquet and natural rivers. Major spring floods were also recorded by *F. nigra* trees from regulated rivers but i) in comparison by very few trees and ii) more often in the form of weakly defined flood rings. The signal strength although appears to decrease with geographical distance to Lake Duparquet and in regulated rivers. The high proportion of individual tree showing significant correlation to the reconstructed Harricana River spring discharge among natural and, to a lesser extent, regulated rivers also support strong spatial coherency. These results confirm the hypothesis of a common hydroclimatic variability among the four river basins sampled. These results are also in line with studies reporting highly significant associations between mean cross-sectional earlywood vessel lumen area (MVA) chronologies from Lake Duparquet and the instrumental regional spring discharge data (Tardif et al., 2010; Kames et al., 2016; Nolin et al., 2021). These results also support the fact that the increase in spring flood frequency and magnitude reported by Nolin et al. (2021) since the end of the Little Ice Age (see their reconstruction of the Harricana River spring discharge) is regionally coherent.

The similarities found at low frequencies in earlywood vessel chronologies also support spatial coherency between Lake Duparquet and natural rivers and point towards a decrease in the periodicities of high spring discharge since at least 1850. The frequency of high spring discharge may have changed from a persistent multi-decadal periodicity in the late 19<sup>th</sup> to early 20<sup>th</sup> century to a decadal and then interannual periodicity in the late 20<sup>th</sup> century. This result compares well with those of previous studies conducted in Lake Duparquet (Tardif & Bergeron, 1997b; Nolin et al., 2021) and hypothesizing a long-term increase in the frequency and magnitude of spring flooding since the end of the Little Ice Age (1850–1870; Matthews & Briffa, 2005). Ideally, the CWT analysis would have been conducted on a large number of samples per river basins to extract the strongest possible common signal, as it was done with the MVA and N chronologies from Lake Duparquet. Indeed, it is possible that factors related to age or stand dynamics may interfere with the hydroclimatic signal in earlywood vessel chronologies (Tardif and Conciatori, 2006b). For example, the sample from upper Ottawa River presented a lot of suppressed years (very small annual ring width) and its MVA chronology was not significantly correlated with that of Lake Duparquet. However, the consistency expressed by the MVA and N chronologies consisting of 1 to 2 trees per river basin compared to the robust Lake Duparquet chronologies (n=43) still demonstrates a strong common signal at both high and low frequencies. It was also demonstrated that five *F. nigra* samples may be sufficient to reconstruct most of the interannual variability of the Harricana River spring discharge during the 20<sup>th</sup> century (EPS > 0.85, Rbar > 0.20; Nolin et al., 2021). Given the similarities observed in the power spectrum of the sampled rivers, it would nevertheless be interesting to conduct this CWT analysis on a larger number of samples and to study their associations with large-scale atmospheric circulations in North America and at different periodicities.

**Table 5**

Pearson's correlation coefficients ( $r$ ) and  $p$  values ( $p$ ) between chronologies of mean lumen cross-sectional area (MVA) and number (N) of earlywood vessels, from four river basins and 10 instrumental records of April 15 to June 30 mean discharge across the study area. The field "Id" is the Canadian federal hydrometric station identification number. The table is ordered by increasing distance between hydrometric stations and Lake Duparquet (left to right) to visualize spatial coherency in the correlation structure. Bold characters denote  $p$  values  $< 0.05$ .

Station			Kinojévis River	Kinojévis River	Blanche River	Harricana River	Porcupine River	Kipawa River	Turgeon River	Missinaibi River	North French River	Missinaibi River
Id			02JB013	02JB003	02JC008	04NA001-2	04MD004	02JE015	04NB001	04LM001	04MF001	04LJ001
Period			1971–2016	1938–1965	1970–2016	1915–2016	1977–2015	1963–2011	1969–1999	1973–2016	1967–2016	1921–2016
N years			46	28	47	102	26	38	24	43	50	96
Distance (km)			30	70	80	85	130	155	170	310	310	320
RECI (1771–2016)	/	$r$	<b>0.86</b>	<b>0.93</b>	<b>0.76</b>	<b>0.82</b>	<b>0.80</b>	<b>0.55</b>	<b>0.73</b>	<b>0.69</b>	<b>0.52</b>	<b>0.57</b>
		$p$	0.0000	0.0000	0.0000	0.0000	0.0000	0.0003	0.0001	0.0000	0.0001	0.0000
Lake Duparquet (1770–2016)	MVA	$r$	<b>-0.83</b>	<b>-0.84</b>	<b>-0.74</b>	<b>-0.78</b>	<b>-0.80</b>	<b>-0.49</b>	<b>-0.76</b>	<b>-0.66</b>	<b>-0.54</b>	<b>-0.56</b>
		$p$	0.0000	0.0000	0.0000	0.0000	0.0000	0.0020	0.0000	0.0000	0.0001	0.0000
	N	$r$	<b>0.67</b>	<b>0.72</b>	<b>0.61</b>	<b>0.62</b>	<b>0.75</b>	0.22	<b>0.64</b>	<b>0.57</b>	<b>0.55</b>	<b>0.46</b>
		$p$	0.0000	0.0000	0.0000	0.0000	0.0000	0.1785	0.0007	0.0001	0.0000	0.0000
Harricana River (1783–2016)	MVA	$r$	<b>-0.84</b>	<b>-0.8</b>	<b>-0.6</b>	<b>-0.81</b>	<b>-0.69</b>	<b>-0.57</b>	<b>-0.57</b>	<b>-0.56</b>	<b>-0.34</b>	<b>-0.49</b>
		$p$	0.0000	0.0000	0.0000	0.0000	0.0001	0.0002	0.0038	0.0001	0.0165	0.0000
	N	$r$	<b>0.47</b>	<b>0.60</b>	<b>0.40</b>	<b>0.53</b>	<b>0.40</b>	0.18	0.17	0.23	<b>0.32</b>	0.24
		$p$	0.0011	0.0007	0.0057	0.0000	0.0428	0.2681	0.4376	0.1320	0.0257	0.0173
Abitibi River (1840–2016)	MVA	$r$	<b>-0.41</b>	<b>-0.49</b>	-0.25	<b>-0.48</b>	<b>-0.65</b>	-0.27	<b>-0.66</b>	<b>-0.61</b>	<b>-0.51</b>	<b>-0.52</b>
		$p$	0.0045	0.0088	0.0969	0.0000	0.0003	0.1052	0.0005	0.0000	0.0002	0.0000
	N	$r$	<b>0.44</b>	<b>0.42</b>	<b>0.48</b>	<b>0.42</b>	<b>0.75</b>	0.21	<b>0.49</b>	<b>0.61</b>	<b>0.44</b>	<b>0.51</b>
		$p$	0.0022	0.0272	0.0006	0.0000	0.0000	0.1988	0.0150	0.0000	0.0013	0.0000
Upper Ottawa River (1814–2016)	MVA	$r$	0.21	-0.44	0.14	-0.18	-0.14	<b>0.42</b>	0.33	0.09	0.17	-0.10
		$p$	0.1563	0.0178	0.3377	0.0645	0.5099	0.0089	0.1197	0.5703	0.2349	0.3172
	N	$r$	0.29	<b>0.53</b>	<b>0.37</b>	<b>0.38</b>	0.33	0.20	0.09	0.13	0.06	<b>0.24</b>
		$p$	0.0523	0.0040	0.0110	0.0001	0.1020	0.2237	0.6710	0.4025	0.6610	0.0189
Mattagami River (1922–2016)	MVA	$r$	-0.07	<b>-0.46</b>	-0.05	<b>-0.22</b>	-0.33	-0.28	0.33	-0.26	-0.12	<b>-0.27</b>
		$p$	0.6510	0.0148	0.7413	0.0305	0.0945	0.0934	0.1100	0.0925	0.3911	0.0084
	N	$r$	<b>0.34</b>	<b>0.45</b>	<b>0.42</b>	<b>0.43</b>	<b>0.45</b>	0.30	0.15	0.42	0.26	<b>0.30</b>
		$p$	0.0215	0.0157	0.0036	0.0000	0.0217	0.0693	0.4914	0.0049	0.0686	0.0036

#### 4.2. Comparison of spring flood proxies among natural rivers, regulated rivers, and unflooded control sites.

Compared to *F. nigra* trees growing along the floodplain of naturally flowing rivers, those from regulated rivers (and from unflooded sites) recorded flood rings less frequently and mainly of the weaker type (F1). Flood-ring chronologies from regulated rivers showed little interannual variability and were also less correlated with hydrometric records. Spring floods identified by flood rings were most coherent with those of natural rivers prior to dam creation in the 1920's and for a few extreme floods thereafter (e.g. 1947, 1960). Some weak flood rings (F1) were also recorded on regulated rivers although they have not been recorded on natural rivers and Lake Duparquet and could be the result of dam management maneuvers. Furthermore, trees were generally younger in floodplain sites located along regulated rivers compared to that along natural rivers and Lake Duparquet, suggesting that the construction of the dams may have had a detrimental effect on the existing ash forests. In hydrological system that were regulated, DeWine and Cooper (2007) demonstrated for instance, that dam construction threatened the recruitment and the persistence of old-growth riparian forests in the upper Colorado River. Historically in Ontario, most dams were built to raise the water level to the high-water mark identified by surveyors using signs on the landscape (Ontario Geological Survey, 1920). Since the dams were built to hold water until the maximum natural flood elevation, it is likely that the old riparian forests have been permanently flooded and removed from the landscape. The potential to accurately reconstruct the historical variability of today's regulated rivers can therefore be lower due to a lack of ancient trees. However, the few trees sampled on the regulated rivers did record flood rings and this demonstrates that flood ring can be suitable proxy to retrieve partial historical discharge records from the trees growing in the shoreline of regulated rivers.

In addition, further work is needed to assess sites differences in regulated hydrological systems. Our results indicated variations in the recording of flood rings by *F. nigra* trees located along lakes regulated by downstream dams (single-dam system) and rivers regulated by both upstream and downstream dams (multi-dam system). It would be interesting to systematically compare flood rings in trees located upstream and downstream of dams, and according to their position on the bank relative to the shoreline, to determine if the hydrological signal provided by flood ring can be improved by a more targeted sampling strategy. Differences in height between dams may also have impacted downstream water levels and flood rings differently.

In the unflooded control sites, the trees were as old as at Lake Duparquet but had little or no flood rings with solely few F1 being observed. The maximum value of F12 never reached more than 10% and flood rings were not consistent among samples. They also did not match the years for which flooding was observed in other river basins, either from the spring flood proxies, the reconstruction of the Harricana River spring discharge or from the regional hydrometric records. This confirms that *F. nigra* trees from flooded and unflooded sites carry different climatic signals, mainly because their exposures to water stress and drought are different (Tardif and Bergeron, 1997a; Kames, 2009). Previous studies in the Lake Duparquet region showed, for example, that earlywood vessel chronologies from unflooded non-riparian *F. nigra* stands were i) not significantly correlated to those developed from flooded riparian stands and ii) presented no significant correlations with instrumental spring discharge (Kames, 2009). This is also sustained by ring-width chronologies developed by Tardif and Bergeron, (1997a) and Kames (2009) showing a lack of crossdating between riparian and non-riparian *F. nigra* trees. The physiological mechanisms of flood-ring formation are still poorly understood, but it was hypothesized that stem submersion induces the production of ethylene which, in turn, interacts with other growth regulators thus affecting the formation of earlywood vessels (Yamamoto et al., 1995; St. George et al., 2002; Copini et al., 2016). It is therefore unlikely that periods of high humidity (runoff,

rainfall, etc.) in topographically flat upland forests will cause a physiological response similar to that of flooding in riparian forests.

#### 4.3. Adequacy between spring flood proxies, advantages and limitations

Spring flood proxies developed in this study (F1, F2, F12, MVA, N) were shown to provide similar and complementary information on high spring discharge variability at an annual resolution. The continuous quantitative measurement of earlywood vessels allowed the extraction of a broader spectrum of hydrological variability compared to the semi-quantitative visual identification of flood rings which provided event-year chronologies.

Among the flood-rings chronologies, F1 and F2 in Lake Duparquet and natural rivers captured very comparable signal but their summation (F12) captured a slightly broader spectrum of hydrological conditions associated with high spring discharge. This result suggest that it is worth identifying both weak (F1) and strong (F2) flood-ring types. It is hypothesized that differences between F1 and F2 in *F. nigra* trees for a given year may be reflecting differences in coring height or tree exposure (elevation and topography) to flooding. In flood years, it has been shown that the decrease in earlywood vessel size is maximum at the base of the trees with a gradual decrease along the trunk height (St. George and Nielsen, 2002; St. George et al., 2002). Furthermore, the timing, intensity and duration of spring floods will also impact the ability of riparian *F. nigra* trees to record a flood ring. St. George et al. (2002) had showed, for instance, that the duration of flooding had a greater influence than the peak flood stage on the size of earlywood vessels in flooded *Quercus macrocarpa*.

Among the anatomical chronologies, MVA and N showed comparable associations to instrumental and reconstructed spring discharge. Although we cannot robustly assert this result given the limited number of samples that have been used, associations between N chronologies and spring discharge were generally higher between river basins and in regulated rivers than with MVA chronologies. It could thus be hypothesized that earlywood vessels area and number carry slightly different hydrological signal associated with spring flooding in natural and regulated rivers. Kames et al. (2016) showed that the MVA and N chronologies extracted from flooded *F. nigra* trees from Lake Duparquet were associated with climate at slightly different periods. The MVA and N chronologies were associated with mean monthly temperatures and total precipitation from April to May and April to June, respectively.

In terms of advantages and limitations, the use of the various spring flood proxies, (F12, MVA or N) depends on the objectives pursued and the resources available (e.g. number of trees, equipment). While quick to develop, visually derived flood-ring chronologies like that of numerous pointer years involve processing a larger number of samples and require conventional dendrochronology equipment (Tardif and Conciatori, 2006a; Therrell and Bialecki, 2015; Meko and Therrell, 2020). Continuous earlywood vessels chronologies require fewer samples but is demanding in image analysis equipment and software, as well as extensive analysis time (Kames et al., 2016, Nolin et al., 2021). Relative frequencies provide information on the number of samples affected per year, while continuous chronologies provide annual quantitative information (Tardif and Conciatori, 2006a). However, it could be hypothesized that, as the number of samples increases, the relative frequency of flood rings could approximate the hydrological signal extracted by earlywood vessel chronologies composed of far fewer samples. It would thus be possible to use relative frequencies of flood rings as spring discharge predictors in reconstruction models, even if conventionally flood-ring frequencies has been used to identify past flooding and not for the purpose of quantitative reconstruction (St. George & Nielsen, 2002; Therrell and Bialecki, 2015; Meko and Therrell, 2020). Examples of approaches combining both discrete and continuous flood proxies to reconstruct spring discharge can be found in Boucher et al. (2011) and in Nicault et al. (2014).



## 5. Conclusion

In a context of climate change, river regulation, and disappearance of old riparian forests, the study of spring flood proxies is becoming a necessity in water management and flood risk assessment in northern territories. This study demonstrated the strong spatial coherency associated with the use of two spring flood proxies in naturally flowing rivers from eastern boreal Canada. It also stressed the potential limitation associated with the use of flood rings from trees growing along regulated water bodies. Flood rings and direct measurement of the earlywood vessels captured high-resolution, comparable, and complementary spring flooding evidence. Even in regulated rivers, partial spring flooding history can be inferred from flood rings prior to dam creation. Results underline the potential and utility of extending the use of these spring flood proxies in dendrohydrology. Future work could study flood rings over a larger area by sampling, for example, one natural river per watershed to monitor historical trends in large-scale spring floods and study the potential effects of climate change. Flood-ring methods could be applied to more southern river basins such as Saint-Lawrence River or Ottawa River. It would then be necessary to study the presence of flood rings in species such as green ash (*Fraxinus pennsylvanica* Marsh.) or potentially in diffuse-porous species.

## Data availability

Relevant data for this study are available from Nolin, A. F., Tardif, J. C., Conciatori, F., & Bergeron, Y. (2021). *Fraxinus nigra* tree-ring dataset for flood history study among major river basins near the Lake Duparquet, eastern boreal Canada. Mendeley Data, v1. <http://dx.doi.org/10.17632/94vjr69fb2.1>. Data include flood ring (F1, F2) and earlywood vessel chronologies (MVA, N) derived from black ash (*Fraxinus nigra* Marsh.) trees growing in eastern boreal Canada near Lake Duparquet (Québec, Canada). F1\_F2\_chrono.csv, as in Fig. 3, the F1 and F2 flood-ring chronologies per sites (sites are coded as in Table 1) with sample replication (n) to reproduce flood-ring frequencies; LAT\_LON.kml, the coordinate data for each site and sampled tree; MVA\_N\_chrono.csv, as in Fig. 5, the MVA and N chronologies per river basins (river basins are coded as in Table 1); REC1.csv, the reconstruction of the Harricana River spring discharge from 1771 to 2016 reported in “Multi-century tree-ring anatomical evidence reveals increasing frequency and magnitude of spring discharge and floods in eastern boreal Canada” published in “Global and Planetary Change” by Nolin et al. 2021. metadatas.txt, a set of self-explanatory instructions and descriptions for data files. All other data are available upon request to the corresponding author at alexandreflorent.nolin@uqat.ca (institutional email), alexandreflorent.nolin@gmail.com (permanent email).

## CRedit authorship contribution statement

**A.F. Nolin:** Conceptualization, Methodology, Investigation, Formal analysis, Writing - original draft, Writing - review & editing, Visualization. **J.C. Tardif:** Conceptualization, Methodology, Investigation, Writing - review & editing, Supervision, Project administration, Funding acquisition. **F. Conciatori:** Methodology, Investigation, Resources, Data curation. **Y. Bergeron:** Conceptualization, Writing - review & editing, Supervision, Project administration, Funding acquisition.

## Declaration of Competing Interest

The authors declare that they have no known competing financial interests or personal relationships that could have appeared to influence the work reported in this paper.

## Acknowledgments

We acknowledge the special support of Mélanie Desrochers (UQAM),

Martin Girardin (CFL), Lars Hildebrandt and Gordon Kayahara (Ontario Forest Service) for their help in the production of the detailed forest maps. We thank field assistants Cyrielle Ducrot, Stéphane Hébert, Chloé Lavelle, Isabelle Gareau, and Ralitsa Mincheva, as well as Johanna M. Robson and Hollie Swart from the University of Winnipeg DendroEcology Lab. We also thank the FERLD research station team and especially Danielle Charron and Raynald Julien for their continuous support over the two summers of field work. This study was a contribution of Canada Research Chairs (NSERC-CRC) hold by YB and JT and was funded by the Natural Sciences and Engineering Research Council of Canada Collaborative research program including our partners Ouranos, Hydro-Québec, Ontario Power Generation (OPG) and The University of Winnipeg. This work was also supported by a scholarship from RIISQ – Intersectorial Flood Network of Québec (2<sup>nd</sup> Program 2020-2021) awarded to AN. Earlier versions of the manuscript benefited from constructive comments by Susanne Kames (U of Winnipeg), Jacinthe Clavet-Gaumont and David Huard (Ouranos), as well as Kurt C. Kornelsen (OPG). We also acknowledge the contributions of the Editor-in-Chief (Pr. Marco Borga) and both reviewers (Pr. Matthew Therrell, and anonymous) who provided constructive comments/suggestions on earlier drafts of the manuscript.

## Appendix A. Supplementary data

Supplementary data to this article can be found online at <https://doi.org/10.1016/j.jhydrol.2021.126084>.

## References

- Agafonov, L.I., Meko, D.M., Panyushkina, I.P., 2016. Reconstruction of Ob River, Russia, discharge from ring widths of floodplain trees. *J. Hydrol.* 543, 198–207. <https://doi.org/10.1016/j.jhydrol.2016.09.031>.
- Aygün, O., Kinnard, C., Campeau, S., 2019. Impacts of climate change on the hydrology of northern midlatitude cold regions. *Prog. Phys. Geogr.: Earth Environ.* 44(3), 338–375. [10.1177/2F0309133319878123](https://doi.org/10.1177/2F0309133319878123).
- Bégin, Y., 2001. Tree-ring dating of extreme lake levels at the subarctic-boreal interface. *Quat. Res.* 55 (2), 133–139. <https://doi.org/10.1006/qres.2000.2203>.
- Berghuijs, W.R., Aalbers, E.E., Larsen, J.R., Trancoso, R., Woods, R.A., 2017. Recent changes in extreme floods across multiple continents. *Environ. Res. Lett.* 12 (11) <https://doi.org/10.1088/1748-9326/aa8847>.
- Biondi, F., Meko, D.M., 2019. Long-term hydroclimatic patterns in the Truckee-Carson basin of the eastern Sierra Nevada, USA. *Water Resour. Res.* 55 (7), 5559–5574. <https://doi.org/10.1029/2019WR024735>.
- Boucher, E., Ouarda, T.B.M.J., Bégin, Y., Nicault, A., 2011. Spring flood reconstruction from continuous and discrete tree ring series. *Water Resour. Res.* 47 (7), W07516. <https://doi.org/10.1029/2010WR010131>.
- Boucher, M.A., Leconte, R., 2013. Changements climatiques et production hydroélectrique canadienne: où en sommes-nous? *Can. Water Resour. J.* 38 (3), 196–209. <https://doi.org/10.1080/07011784.2013.818297>.
- Bunn, A.G., 2008. A dendrochronology program library in R (dplR). *Dendrochronologia* 26 (2), 115–124. <https://doi.org/10.1016/j.dendro.2008.01.002>.
- Burn, D.H., Whitfield, P.H., 2016. Changes in floods and flood regimes in Canada. *Can. Water Resour. J.* 41 (1–2), 139–150. <https://doi.org/10.1080/07011784.2015.1026844>.
- Bush, E., Lemmen, D.S. (Eds.), 2019. *Canada's Changing Climate Report*. Government of Canada, Ottawa, ON, Canada, p. 444p.
- Canny, J., 1986. A computational approach to edge detection. *IEEE Trans. Pattern Anal. Mach. Intell.* PAMI-8(6), 679–698. <https://doi.org/10.1109/TPAMI.1986.4767851>.
- Centre d'Expertise Hydrique du Québec (CEHQ), 2019. Répertoire des barrages. Ministère de l'Environnement et de la Lutte contre les Changements climatiques. Gouvernement du Québec, Ottawa. Retrieved from: <https://www.cehq.gouv.qc.ca/barrages/default.asp> [February 12, 2020].
- Cherry, J.E., Knapp, C., Trainor, S., Ray, A.J., Tedesche, M., Walker, S., 2017. Planning for climate change impacts on hydropower in the Far North. *Hydrol. Earth Syst. Sci.* 21 (1), 133–151. <https://doi.org/10.5194/hess-21-133-2017>.
- Clavet-Gaumont, J., Huard, D., Frigon, A., Koenig, K., Slota, P., Rousseau, A., Klein, I., Thiémondge, N., Houdré, F., Perdikaris, J., Turcotte, R., Lafleur, J., Larouche, B., 2017. Probable maximum flood in a changing climate: An overview for Canadian basins. *J. Hydrol.: Reg. Stud.* 13 (July), 11–25. <https://doi.org/10.1016/j.ejrh.2017.07.003>.
- Copini, P., Den Ouden, J., Robert, E.M.R., Tardif, J.C., Loesberg, W.A., Goudzwaard, L., Sass-Klaassen, U., 2016. Flood ring formation and root development in response to experimental flooding of young *Quercus robur* trees. *Front. Plant Sci.* 7 (June), 1–14. <https://doi.org/10.3389/fpls.2016.00775>.
- Cook, E.R., Kairiukstis, L.A., 1990. *Methods of Dendrochronology: Applications in the Environmental Sciences* (Springer (ed.)). International Institute for Applied System Analysis, Kluwer Academic, Boston, 394p. ISBN: 978-94-015-7879-0.

- Daubois, V., Roy, M., Veillette, J.J., Ménard, M., 2015. The drainage of Lake Ojibway in glaciolacustrine sediments of northern Ontario and Quebec, Canada. *Boreas* 44 (2), 305–318. <https://doi.org/10.1111/bor.12101>.
- DeWine, J.M., Cooper, D.J., 2007. Effects of river regulation on riparian box elder (*Acer negundo*) forests in canyons of the Upper Colorado River Basin, USA. *Wetlands* 27 (2), 278–289.
- Denneler, B., Bergeron, Y., Bégin, Y., 1999. An attempt to explain the distribution of the tree species composing the riparian forests of Lake Duparquet, southern boreal region of Quebec, Canada. *Can. J. Botany* 77 (12), 1744–1755. <https://doi.org/10.1139/cjb-77-12-1744>.
- Déry, S.J., Mlynowski, T.J., Hernández-Henríquez, M.A., Straneo, F., 2011. Interannual variability and interdecadal trends in Hudson Bay streamflow. *J. Mar. Syst.* 88 (3), 341–351. <https://doi.org/10.1016/j.jmarsys.2010.12.002>.
- Environment and Climate Change Canada, 2020. Canada's top 10 weather stories of 2019. Government of Canada, Toronto, Canada. Retrieved from: <https://www.canada.ca/en/environment-climate-change/services/top-ten-weather-stories/2019.html#toc2> [1 Sept 2020].
- Gaur, A., Gaur, A., Simonovic, S.P., 2018. Future changes in flood hazards across Canada under a changing climate. *Water (Switzerland)* 10 (10), 1441. <https://doi.org/10.3390/w10101441>.
- Gouhier, T.C., Grinsted, A., Simko, V., 2019. Package 'biwavelet'. Conduct univariate and bivariate wavelet analyses. R-package version 0.20.19. <https://cran.r-project.org/web/packages/biwavelet/biwavelet.pdf>.
- Griffin, D., Woodhouse, C.A., Meko, D.M., Stahle, D.W., Faulstich, H.L., Carrillo, C., Touchan, R., Castro, C.L., Leavitt, S.W., 2013. North American monsoon precipitation reconstructed from tree-ring latewood. *Geophys. Res. Lett.* 40 (5), 954–958. <https://doi.org/10.1002/grl.50184>.
- Guay, C., Minville, M., Braun, M., 2015. A global portrait of hydrological changes at the 2050 horizon for the province of Québec. *Can. Water Resour. J.* 40 (3), 285–302. <https://doi.org/10.1080/07011784.2015.1043583>.
- Harrell, F.E., 2020. Hmisc: Harrell Miscellaneous. R package version 4.4-0. <https://cran.r-project.org/web/packages/Hmisc/Hmisc.pdf>.
- Holmes, R.L., 1983. Computer-assisted quality control in tree-ring dating and measurement - COFECHA. *Tree-Ring Bull.* 43, 69–78.
- Hydro-Québec, 2020. Annual Report 2019. Report n° 2019G500A. Bibliothèque et Archives nationales du Québec. Montréal, Québec, Canada. 177p. <https://www.hydr.quebec.com/data/documents-donnees/pdf/annual-report.pdf>.
- Insurance Bureau of Canada (IBC), 2020. Investing in Canada's Future; The Cost of Climate Adaptation at the Local Level. Final report (February 2020). Federation of the Canadian Municipalities, 59p.
- Intergovernmental Panel on Climate Change (IPCC), 2018. Global Warming of 1.5°C. An IPCC Special Report on the impacts of global warming [Masson-Delmotte, V., P. Zhai, H.-O. Pörtner, D. Roberts, J. Skea, P.R. Shukla, A. Pirani, W. Moufouma-Okia, C. Péan, R. Pidcock, S. Connors, J.B.R. Matthews, Y. Chen, X. Zhou, M.I. Gomis, E. Lonnoy, T. Maycock, M. Tignor, and T. Waterfield (eds.)].
- Kames, S., 2009. Sensitivity of vessels in black ash (*Fraxinus nigra* Marsh.) tree rings to fire and hydro-climatic variables. (Master's Thesis, University of Manitoba, Canada). 174p. Retrieved from: [https://mspace.lib.umanitoba.ca/bitstream/handle/1993/3216/KAMES\\_Thesis\\_Final.pdf?sequence=1](https://mspace.lib.umanitoba.ca/bitstream/handle/1993/3216/KAMES_Thesis_Final.pdf?sequence=1).
- Kames, S., Tardif, J.C., Bergeron, Y., 2016. Continuous earlywood vessels chronologies in floodplain ring-porous species can improve dendrohydrological reconstructions of spring high flows and flood levels. *J. Hydrol.* 534, 377–389. <https://doi.org/10.1016/j.jhydrol.2016.01.002>.
- Kundzewicz, Z.W., Szwed, M., Pińskwar, I., 2019. Climate variability and floods - A global review. *Water (Switzerland)* 11 (7). <https://doi.org/10.3390/w11071399>.
- Larsson, L.-A., 2003. CDendro: Cybis Dendro dating program. Available at: <http://www.cybis.se>.
- Legendre, P., Legendre, L., 2012. Numerical Ecology (Development) 3rd Edition. Elsevier, 1006p. ISBN: 978444538680.
- Matthews, J.A., Briffa, K.R., 2005. The 'Little Ice Age': re-evaluation of an evolving concept. *Geografiska Ann.: Ser. A, Phys. Geogr.* 87 (1), 17–36. <https://doi.org/10.1111/j.0435-3676.2005.00242.x>.
- Meko, D.M., Woodhouse, C.A., 2011. Application of streamflow reconstruction to water resources management. In: *Dendroclimatology, developments in paleoenvironmental research*, 11. Springer, Dordrecht, pp. 231–261. <https://doi.org/10.1007/978-1-4020-5725-0>.
- Meko, M.D., Therrell, M.D., 2020. A record of flooding on the White River, Arkansas derived from tree-ring anatomical variability and vessel width. *Phys. Geogr.* 41 (1), 83–98. <https://doi.org/10.1080/02723646.2019.1677411>.
- Mortsch, L., Cohen, S., Koshida, G., 2015. Climate and water availability indicators in Canada: Challenges and a way forward. Part II – Historic trends. *Can. Water Resour. J./Rev. canadienne des ressources hydriques* 40 (2), 146–159. <https://doi.org/10.1080/07011784.2015.1006024>.
- Mudryk, L.R., Derksen, C., Howell, S., Laliberté, F., Thackeray, C., Sospedra-Alfonso, R., Vionnet, V., Kushner, P.J., Brown, R., 2018. Canadian snow and sea ice: historical trends and projections. *The Cryosphere* 12 (4), 1157. <https://doi.org/10.5194/tc-12-1157-2018>.
- Netsvetov, M., Prokopyuk, Y., Puchalka, R., Koprowski, M., Klisz, M., Romensky, M., 2019. River regulation causes rapid changes in relationships between floodplain oak growth and environmental variables. *Front. Plant Sci.* 10, 96. <https://doi.org/10.3389/fpls.2019.00096>.
- Nicault, A., Boucher, E., Bégin, C., Guiot, J., Marion, J., Perreault, L., Roy, R., Savard, M., Bégin, Y., 2014. Hydrological reconstruction from tree-ring multi-proxies over the last two centuries at the Caniapiscau Reservoir, northern Québec, Canada. *J. Hydrol.* 513, 435–445. <https://doi.org/10.1016/j.jhydrol.2014.03.054>.
- Nolin, A.F., Tardif, J.C., Conciatori, F., Kames, S., Meko, D.M., Bergeron, Y., 2021. Multi-century tree-ring anatomical evidence reveals increasing frequency and magnitude of spring discharge and floods in eastern boreal Canada. *Global and Planetary Change* 199, 103444. <https://doi.org/10.1016/j.gloplacha.2021.103444>.
- Ontario Geological Survey (OGS), 1920. Twenty-ninth annual report of the Ontario Department of Mines. Vol. XXIX, Part I to VI, (1920), 664p. Ryerson Press, Toronto, Ontario. Retrieved from: <http://www.geologyontario.mndmf.gov.on.ca/mndmfiles/pub/data/imaging/ARV29/ARV29.pdf> [January 21, 2021].
- Ontario Ministry of Natural Resources and Forestry (OMNRF), 2019. Ontario Dam Inventory, Provincial Mapping Unit, Government of Ontario, Toronto. Retrieved from: <https://geohub.lio.gov.on.ca/datasets/mnrf:ontario-dam-inventory> [February 12, 2020].
- Phipps, R.L., 1985. Collecting, preparing, crossdating, and measuring tree increment cores. U.S. Geological Survey. Water Resources Investigations Report 85–4148, 48p. <https://doi.org/10.3133/wri854148>.
- R Core Team, 2020. R: A language and environment for statistical computing. R Foundation for Statistical Computing, Vienna, Austria <http://www.R-project.org/>.
- Régent Instruments Inc, 2018. WinCell Pro Version 2018c user manual. Québec, Québec.
- Reily, P.W., Johnson, W.C., 1981. The effects of altered hydrologic regime on tree growth along the Missouri River in North Dakota. *Can. J. Botany* 60 (11), 2410–2423. <https://doi.org/10.1139/b82-294>.
- Rueden, C.T., Schindelin, J., Hiner, M.C., DeZonia, B.E., Walter, A.E., Arena, E.T., Elceiri, K.W., 2017. ImageJ2: ImageJ for the next generation of scientific image data. *BMC Bioinform.* 18 (529), 1–26. <https://doi.org/10.1186/s12859-017-1934-z>.
- Schook, D.M., Friedman, J.M., Rathburn, S.L., 2016. Flow reconstructions in the Upper Missouri River Basin using riparian tree rings. *Water Resour. Res.* 52 (10), 8159–8173. <https://doi.org/10.1002/2016WR018845>.
- Stella, J.C., Bendix, J., 2019. Multiple stressors in riparian ecosystems, in *Multiple Stressors in River Ecosystems. Status, impacts and prospects for the future* [S. Sabater, A. Elosegi, and R. Ludwig (eds.)], (New York, Elsevier), 81–110.
- St. George, S., Nielsen, E., 2000. Signatures of high-magnitude 19th-century floods in Quercus macrocarpa tree rings along the Red River, Manitoba, Canada. *Geology*, 28 (10), 899–902. [https://doi.org/10.1130/0091-7613\(2000\)28<899:SOHTFI>2.0.CO;2](https://doi.org/10.1130/0091-7613(2000)28<899:SOHTFI>2.0.CO;2).
- St. George, S., Nielsen, E., 2002. Flood Ring Evidence and its Application to Paleoflood Hydrology of the Red River and Assiniboine River in Manitoba. *Géogr. Phys. Quat.* 56(2–3), 181. <https://doi.org/10.7202/009104ar>.
- St. George, S., Nielsen, E., Conciatori, F., Tardif, J., 2002. Trends in Quercus macrocarpa vessel area and their implications for tree-ring paleoflood studies. *Tree-Ring Res.* 58, 3–10.
- St. George, S., Nielsen, E., 2003. Paleoflood records for the Red River, Manitoba, Canada, derived from anatomical tree-ring signatures. *The Holocene*, 13(4), 547–555. <https://doi.org/10.1191/0959683603hl645rp>.
- Tardif, J.C., Bergeron, Y., 1992. Analyse écologique des peuplements de frêne noir (*Fraxinus nigra*) des rives du lac Duparquet, nord-ouest du Québec. *Can. J. Botany* 70 (11), 2294–2302. <https://doi.org/10.1139/b92-285>.
- Tardif, J.C., Bergeron, Y., 1997a. Comparative dendroclimatological analysis of two black ash and two white cedar populations from contrasting sites in the Lake Duparquet region, northwestern Quebec. *Can. J. For. Res.* 27, 108–116. <https://doi.org/10.1139/x96-150>.
- Tardif, J.C., Bergeron, Y., 1997b. Ice-flood history reconstructed with tree-rings from the southern boreal forest limit, western Quebec. *The Holocene* 7 (3), 291–300. <https://doi.org/10.1177/095968369700700305>.
- Tardif, J.C., Conciatori, F., 2006a. A comparison of ring-width and event-year chronologies derived from white oak (*Quercus alba*) and northern red oak (*Quercus rubra*), southwestern Quebec. *Canada. Dendrochronologia* 23 (3), 133–138. <https://doi.org/10.1016/j.dendro.2005.10.001>.
- Tardif, J., Conciatori, F., 2006b. Influence of climate on tree rings and vessel features in red oak and white oak growing near their northern distribution limit, southwestern Québec, Canada. *Can. J. For. Res.* 36, 2317–2330. <https://doi.org/10.1139/x06-133>.
- Tardif, J.C., Kames, S., Bergeron, Y., 2010. Spring water levels reconstructed from ice-scarred trees and cross-sectional area of the earlywood vessels in tree rings from eastern boreal Canada. *Tree Rings Nat. Hazards* 257–261. [https://doi.org/10.1007/978-90-481-8736-2\\_24](https://doi.org/10.1007/978-90-481-8736-2_24).
- Torrence, C., Compo, G.P., 1998. A practical guide to wavelet analysis. *Bull. Am. Meteorol. Soc.* 79 (1), 61–78. [https://doi.org/10.1175/1520-0477\(1998\)079%3C0061:APGTWA%3E2.0.CO;2](https://doi.org/10.1175/1520-0477(1998)079%3C0061:APGTWA%3E2.0.CO;2).
- Therrell, M.D., Bialecki, M.B., 2015. A multi-century tree-ring record of spring flooding on the Mississippi River. *J. Hydrol.* 529 (P2), 490–498. <https://doi.org/10.1016/j.jhydrol.2014.11.005>.
- Vincent, L.A., Zhang, X., Brown, R.D., Feng, Y., Mekis, E., Milewska, E.J., Wang, X., Wang, X.L., 2015. Observed trends in Canada's climate and influence of low-frequency variability modes. *J. Clim.* 28 (11), 4545–4560. <https://doi.org/10.1175/JCLI-D-14-00697.1>.
- Wertz, E. L., St. George, S., Zeleznik, J.D., 2013. Vessel anomalies in Quercus macrocarpa tree rings associated with recent floods along the Red River of the North, United States. *Water Resour. Res.* 49(1), 630–634. <https://doi.org/10.1029/2012WR012900>.
- Yamamoto, F., Sakata, T., Terazawa, K., 1995. Physiological, morphological and anatomical responses of Fraxinus mandshurica seedlings to flooding. *Tree Physiol.* 15(11), 713–9. <https://doi.org/10.1093/treephys/15.11.713>.
- Zhang, X., Vincent, L.A., Hogg, W.D., Niitsoo, A., 2000. Temperature and precipitation trends in Canada during the 20<sup>th</sup> century. *Atmos.-Ocean* 38 (3), 395–429. <https://doi.org/10.1080/07055900.2000.9649654>.